RSC Advances

PAPER

View Article Online
View Journal | View Issue

Cite this: *RSC Adv.*, 2016, **6**, 47454

Efficient inverted polymer solar cells employing an aqueous processing RbF cathode interfacial layer

Fengyuan Lin,[ab] Xiaoyang Guo,*[a] Yongsheng Hu,[a] Yantao Li[a] and Xingyuan Liu*[a]

Received 11th April 2016
Accepted 6th May 2016

DOI: 10.1039/c6ra09272a

www.rsc.org/advances

In this work, for the first time, thermal evaporated rubidium fluoride (RbF) and water-soluble RbF have been employed as the cathode interfacial layers (CILs) in inverted polymer solar cells (PSCs), respectively. The device with thermal evaporated RbF CIL exhibited a power conversion efficiency (PCE) of 6.41% when the thickness of RbF was 14 Å. A higher PCE of 6.82% was obtained in the aqueous RbF-based device, which is higher than that of a typical ZnO-CIL-based device (6.73%). More importantly, aqueous RbF opens a route to less poisonous, convenient, and low-cost processing CIL in inverted PSCs.

1. Introduction

Bulk heterojunction polymer solar cells (PSCs) based on blends of conjugated polymers and fullerene derivatives have been widely studied over the past few years because of their low cost, flexibility, renewability, and large-area processing. In recent years, power conversion efficiency (PCE) of single-junction PSCs has reached over 10%.[1–3] In traditional PSC devices, indium-tin oxide (ITO) appears as a transparent anode generally, and poly(3,4-ethylenedioxythiophene):poly(styrene-sulfonate) (PEDOT:PSS) is often used as an anode interfacial layer to modify the morphology of ITO, promote the work function of the anode and ensure ohmic contact.[4–6] However, the acidic PEDOT:PSS may corrode the surface of the ITO anode and cause the diffusion of indium into the active layer and the degradation of PSC performance.[7–9] Additionally, the optical losses in PEDOT:PSS in conventional devices decreased the light irradiating on the active layers. Therefore, an inverted architecture, reversing the charge collection nature, has been proposed, which can avoid the negative influence of PEDOT:PSS at the ITO interface and increase the light absorption and stability of the PSC devices.[10–12]

In the inverted PSCs, low work function and transparent cathode interfacial layer (CIL) coated ITO is required to serve as the cathode, and some high work function transition metal oxides, such as MoO_3,[13,14] WO_3,[15] NiO,[16] and V_2O_5 [17,18] to be used as hole extraction layers at anode. For the CIL materials, low work function and transparent metal oxides such as ZnO_x [19] and TiO_x [20] have been used to facilitate efficient electron extraction from the active layer to the ITO electrode. However, these CILs often introduce the "light-soaking" problem, which is generally considered to be caused by the interface problem due to the metal oxide. Usually, performance of the device is poor in the immediate test after preparation, the current density–voltage (*J*–*V*) characteristic curve presents abnormal "S" type. The situation would be ameliorated when device is irradiated under continuous light.[21,22]

In conventional PSC devices, ultrathin metal fluorides, such as LiF,[23] CsF,[24] and BaF_2,[25] have usually been introduced as CILs at metal electrodes, which can be thermal evaporated together with the metal electrode in succession. But metal fluorides have seldom been used at the ITO electrodes, which is mainly due to its inconvenient processing with the solution processed active layers and difficult control of its ultrathin thickness under thermal evaporation. Herein, a water-soluble metal fluoride–rubidium fluoride (RbF) has been employed as the CIL at the ITO electrode in the inverted PSC devices for the first time. The devices with thermal evaporated RbF as the CIL have also been prepared. The device with thermal evaporated RbF CIL exhibited a PCE of 6.41%, while a higher PCE of 6.82% was obtained in the device with aqueous prepared RbF CIL, equivalent to that of ZnO CIL-based devices. The compatible solution processing technique suggests that aqueous RbF can be used as a less poisonous and low-cost CIL for inverted PSC devices.

2. Experimental

2.1 Preparation of CIL solution

(1) Butanol solution of ZnO: first of all, dissolve 1.23 g $Zn(Ac)_2 \cdot 2H_2O$ (Sigma-Aldrich) in 55 mL methanol at room temperature. Then, a 25 mL methanol solution containing 0.48 g KOH was added dropwise at 60 °C with magnetic stirring. The reaction mixture was maintained at 60 °C under N_2 atmosphere for 2 h. Collect the white precipitate product by centrifugation and then wash with methanol. Finally, the precipitate was redispersed in butanol by 20 mg mL^{-1} for further experiment. (2) Aqueous solution of RbF: RbF (Alfa Aesar) dissolved in

[a]State Key Laboratory of Luminescence and Applications, Changchun Institute of Optics, Fine Mechanics and Physics, Chinese Academy of Sciences, Changchun 130033, China. E-mail: guoxy@ciomp.ac.cn; liuxy@ciomp.ac.cn
[b]University of Chinese Academy of Sciences, Beijing 100049, China

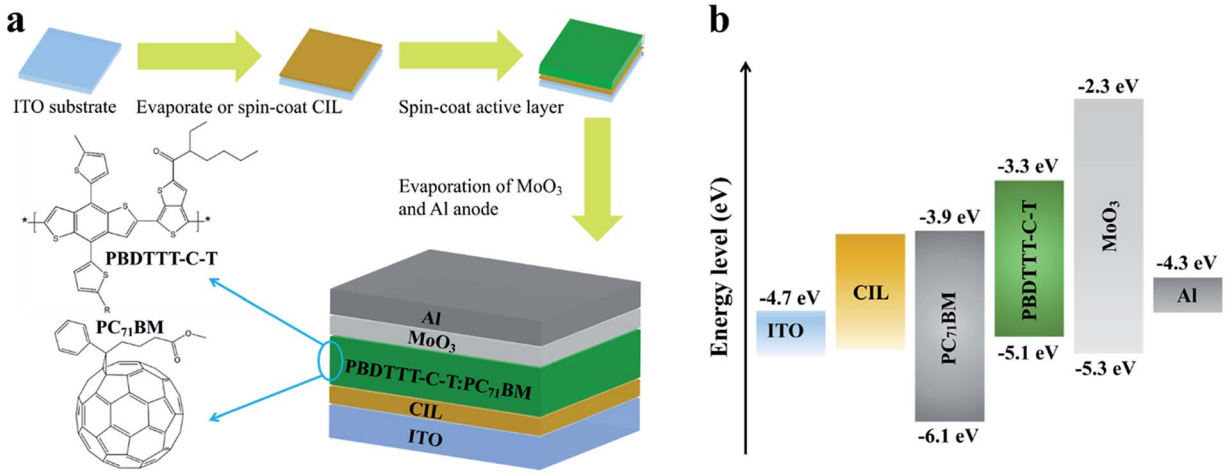

Fig. 1 (a) The production process and architecture of the inverted PSC device. (b) The energy level diagram of the inverted PSC.

deionized water according to the ratio of 1.5 wt‰, 2.0 wt‰, 2.5 wt‰, 3.0 wt‰, 3.5 wt‰, 4.0 wt‰, 4.5 wt‰, and then ultrasonic treated until dissolved fully.

2.2 Device fabrication

The architecture of the inverted PSC including production process and the energy level alignment of the materials used in this work are shown in Fig. 1. The widely used transparent ITO was utilized as the bottom cathode, which was cleaned with acetone, alcohol, and deionized water in an ultrasonic bath and then placed in a vacuum drying oven to remove moisture. Next, the ITO substrates were coated with evaporation deposited RbF (1 Å s^{-1}), spin-coated RbF (2500 rpm) or ZnO (2000 rpm). And then, the samples with spin-coated RbF or ZnO were heated on a hot plate at 120 °C for 10 min to eliminate residual water or solvent. Subsequently, the samples were transferred into a N_2 glove box. A blend of a low-band gap conjugated polymer, poly [4,8-bis-substituted-benzo[1,2-*b*:4,5-*b*′]dithiophene-2,6-diyl-*alt*-4-substituted-thieno[3,4-*b*]thiophene-2,6-diyl] (PBDTTT-C-T, Solarmer Materials Inc.), and [6,6]-phenyl C_{71}-butyric acid methyl ester ($PC_{71}BM$, American Dye Source Inc.) in a 1 : 1.5 ratio by weight was spin-coated onto the samples from 1,2-dichlorobenzene (Sigma-Aldrich) for use as the active layer (800 rpm, *ca.* 100 nm). A small amount (3 vol%) of a high-boiling point additive, 1,8-diiodooctane (DIO, Sigma-Aldrich), was used to optimize the morphology of the active layer. Finally, MoO_3 (20 nm) and Al (100 nm) were thermally deposited in vacuum at a pressure of 2.5×10^{-4} Pa. The active area of the inverted PSC devices was 0.12 cm^2. All measurements were carried out in air without encapsulation.

2.3 Characterization

Film thicknesses were measured with an Ambios XP-1 surface profiler. The *J*–*V* characteristics of PSCs were measured using a computer-controlled Keithley 2611 source meter under AM 1.5G illumination from a calibrated solar simulator with an irradiation intensity of 100 mW cm^{-2} and in the dark. External quantum efficiency (EQE) measurements were performed with a lock-in amplifier at a chopping frequency of 20 Hz under illumination with monochromatic light from a xenon lamp. Ultraviolet photoelectron spectroscopy (UPS) were obtained using a Thermo Fisher Scientific Ultra Spectrometer ESCALAB 250 surface analysis system equipped with a helium discharge lamp ($h\nu$ = 21.22 eV) and a bias of −8.0 V was applied to the samples. Atomic force microscope (AFM) measurements were performed on a Shimadzu SPM-9700 (Shimadzu Corp., Japan) in tapping mode.

3. Results and discussion

Firstly, the feasibility of evaporated RbF layers as the CIL was experimentally validated in the inverted PSCs. The *J*–*V* characteristics of these PSCs under AM 1.5G irradiation at 100 mW cm^{-2} are shown in Fig. 2a, and the device parameters are listed in Table 1. When the RbF thickness is 14 Å, device exhibited the highest PCE of 6.41% with an open circuit voltage (V_{OC}) of 0.75 V, a short circuit current density (J_{SC}) of 14.96 mA cm^{-2}, and a fill factor (FF) of 57.12%. For comparing, devices without CIL and with ZnO as the CIL were also fabricated and shown in Fig. 2a and Table 1, respectively. The device without CIL shows a PCE of 1.37% together with a V_{OC} of 0.33 V, a J_{SC} of 14.70 mA cm^{-2} and a FF of 28.20%. The device with ZnO as the CIL exhibits a PCE of 6.73% with a V_{OC} of 0.76 V, a J_{SC} of 14.99 mA cm^{-2} and a FF of 59.08%. The series resistance (R_s) and sheet resistance (R_{sh}) of the devices with different CILs were calculated from the *J*–*V* characteristics and listed in Table 1. The device with 14 Å RbF as the CIL shows a small R_s of 7.50 Ω cm^2 and a relative higher R_{sh} of 769.23 Ω cm^2, indicating a modified ohmic contact at the ITO/RbF interface, which are comparable with those of ZnO-based device. But the lower FF results in a lower PCE of the RbF-based device in comparison with the ZnO-based device. Although the performance of RbF-based device is slightly lower than the ZnO-based device, the evaporation deposited RbF-based device shows a minimum R_s, a higher R_{sh}, and obtains a PCE of 3.68 times higher than that of

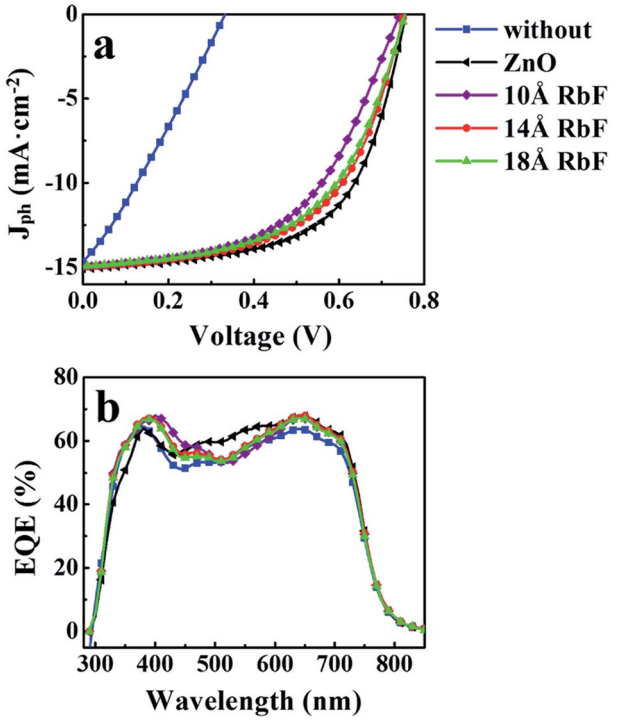

Fig. 2 (a) J–V characteristics of the PSCs with evaporation deposited RbF CIL under AM 1.5G irradiation at 100 mW cm^{-2}. (b) EQE spectra of the PSCs with evaporation deposited RbF CIL. Devices without CIL and with ZnO CIL are also shown as references.

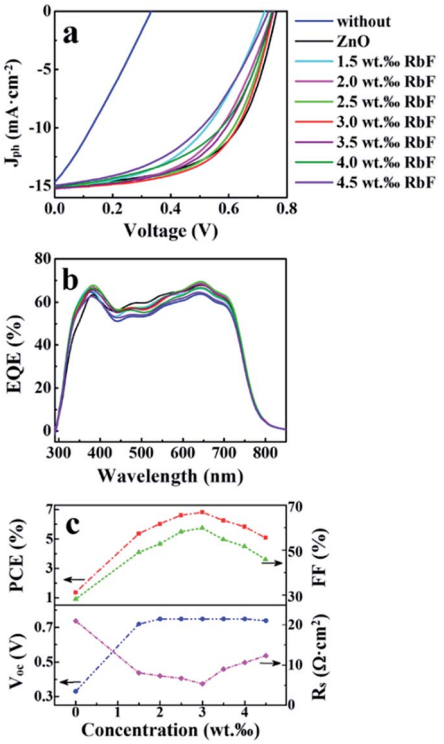

Fig. 3 (a) J–V characteristics of the PSCs with RbF CIL prepared by aqueous solutions with different concentrations under AM 1.5G irradiation at 100 mW cm^{-2}. (b) EQE spectra of the PSCs with RbF CIL prepared by aqueous solutions with different concentrations. (c) The dependence of PCE, FF, V_{OC}, and R_s of the PSCs on the concentration of RbF aqueous solution.

PSC without CIL, indicating that RbF is a useful CIL candidate for inverted PSC devices. The EQE spectra of these PSCs are shown in Fig. 2b, and the J_{SC} calculated by EQE spectra are also listed in Table 1, which are consistent with the values measured by J–V test.

Furthermore, we found that RbF is easily soluble in water indicating that very thin RbF CIL layer can be prepared by spin coating. Inverted PSCs based on RbF CIL with different RbF aqueous solution concentrations were fabricated. Fig. 3a shows the J–V characteristics of the PSCs with aqueous RbF as the CILs under AM 1.5G irradiation at 100 mW cm^{-2}, and the device parameters are listed in Table 2. With the change of aqueous solution concentration of RbF from 1.5 to 4.5 wt‰, all the device performance parameters improve firstly and then deteriorate, the variation tendency has been shown in Fig. 3c. When the aqueous solution concentration of RbF increases from 0 to 3.0 wt‰, V_{OC} increases from 0.33 V to 0.75 V, FF increases from 28.20% to 59.84%, R_s decreases from 21.04 Ω cm^2 to 5.34 Ω cm^2, R_{sh} increases from 35.74 Ω cm^2 to 781.25 Ω cm^2, and thus PCE comes to a maximum of 6.82% with a V_{OC} of 0.75 V, a J_{SC} of 15.19 mA cm^{-2}, and a FF of 59.84%. But as the RbF aqueous concentration further increasing, the R_s begins to increase due to the insulating nature of RbF, and resulting in a gradually decreased PCE. The EQE spectra of these PSCs are shown in Fig. 3b, and the J_{SC} calculated by EQE spectra are also listed in Table 2, which are consistent with the values measured by J–V test. Compared with the thermal evaporated RbF-based device, the aqueous RbF-based device shows a higher PCE, which is even higher than that of the ZnO-based device. And both of the thermal evaporated and aqueous RbF-based devices have no "light-soaking" problem, which is generally found in ZnO-based devices.

Table 1 Performance parameters of PSCs without CIL, with ZnO CIL, and evaporated RbF CIL

CIL	Thickness [Å]	J_{SC} calculated by EQE [mA cm^{-2}]	V_{OC} [V]	J_{SC} [mA cm^{-2}]	FF [%]	R_s [Ω cm^2]	R_{sh} [Ω cm^2]	PCE [%]
Without	0	14.04	0.33	14.70	28.20	21.04	35.74	1.37
ZnO	100	14.96	0.76	14.99	59.08	5.42	448.43	6.73
RbF	10	14.68	0.74	14.98	52.79	19.69	625.00	5.85
RbF	14	14.79	0.75	14.96	57.12	7.50	769.23	6.41
RbF	18	14.60	0.75	14.95	55.43	9.03	793.65	6.22

Table 2 Performance parameters of PSCs with RbF CILs prepared with different aqueous solution concentrations (0 wt‰ means without CIL)

Concentration of RbF aqueous solution [wt‰]	J_{SC} calculated by EQE [mA cm^{-2}]	V_{OC} [V]	J_{SC} [mA cm^{-2}]	FF [%]	R_s [Ω cm^2]	R_{sh} [Ω cm^2]	PCE [%]
0	14.04	0.33	14.70	28.20	21.04	35.74	1.37
1.5	14.89	0.72	15.19	49.03	8.07	421.94	5.36
2.0	15.10	0.75	15.25	52.79	7.32	500.00	6.04
2.5	15.18	0.75	15.15	58.18	6.71	606.06	6.61
3.0	15.02	0.75	15.19	59.84	5.34	781.25	6.82
3.5	14.93	0.75	15.22	54.74	9.01	526.32	6.26
4.0	14.70	0.75	15.07	51.63	10.68	434.78	5.84
4.5	14.20	0.74	14.99	45.85	12.35	289.86	5.09

In order to further study the effect of RbF CIL layer on the device, UPS and AFM were carried out and the results are shown in Fig. 4 and 5, respectively. From Fig. 4, effective work function (φ) of different cathodes can be calculated through the following equations,[26,27]

$$\varphi = 21.22\ \text{eV} - E_{\text{cutoff}} + E_{\text{Fermi}} \quad (1)$$

where, E_{cutoff} and E_{Fermi} were extracted in Fig. 4 (the detailed method has been reported in ref. 26) and marked in the inset of Fig. 4. Effective work functions of ITO and ITO/ZnO are 4.73 eV and 4.33 eV, respectively, coincided with the previously reported data.[9,19,28] Meanwhile, effective work functions of ITO with evaporated RbF and aqueous RbF coated ITO electrode are 3.20 eV and 3.03 eV, respectively. The work function of ZnO or RbF modified ITO matches well with the lowest unoccupied molecular orbital (LUMO) of the $PC_{71}BM$ (3.9 eV) as shown in Fig. 1b, resulting in effective electron extraction at cathode, and then enhanced V_{OC} and PCE.

Fig. 5 shows the AFM images of ITO substrate, evaporation deposited RbF (14 Å) and spin-coated RbF (3.0 wt‰) on ITO substrate. The root-mean-square (RMS) roughness of these samples is 2.065 nm, 2.956 nm and 1.702 nm, respectively. The RMS of ITO/evaporated RbF is higher than that of the pure ITO, resulting from the island growth of the discontinuous RbF film, which results in a lower FF in the ITO/RbF (evaporated 14 Å) based device (Table 1). But the ITO/spin-coated RbF shows a lower RMS, which indicates that the aqueous RbF can fill the defect area of ITO surface and smooth ITO substrate. Therefore, the aqueous RbF-based device shows a lower R_s than that of the evaporated RbF-based device, leading to higher FF and PCE in the aqueous RbF-based PSCs.

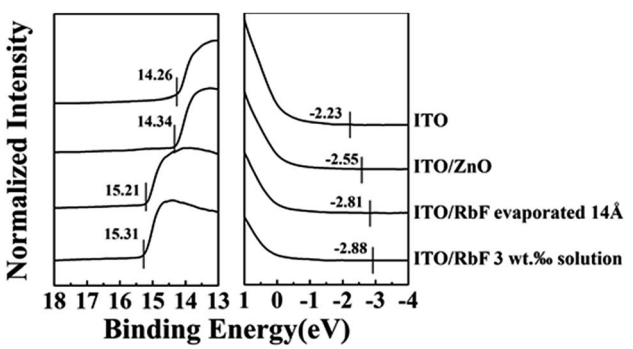

Fig. 4 E_{cutoff} and E_{Fermi} regions of ITO, ITO/ZnO, ITO/RbF (evaporated 14 Å), and ITO/RbF (3 wt‰ aqueous solution).

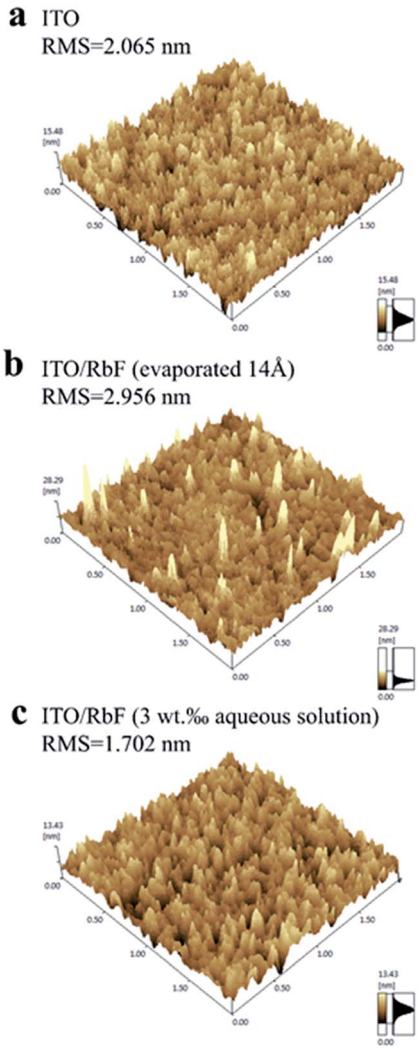

Fig. 5 AFM images of (a) ITO, (b) ITO/RbF (evaporated 14 Å), and (c) ITO/RbF (spin-coated from 3 wt‰ aqueous solution).

4. Conclusions

A metal fluoride, RbF, has been introduced as a cathode interface layer in the inverted PSC devices. It is found that RbF layer can be deposited not only by thermal evaporation, but also spin coating from aqueous solution. Comparing with conventional ZnO-based PSC devices, devices based on thermal evaporated RbF and aqueous RbF show similar PCEs of 6.41% and 6.82%, respectively, but without "light-soaking" problem. The effective function as cathode interface layer and the compatible room-temperature solution processing technique with PSCs indicates that aqueous RbF have promising application in low-cost and large-area processing inverted PSC devices.

Acknowledgements

This work is supported by the CAS Innovation Program, the National Natural Science Foundation of China No. 61106057 and 6140031454, the Jilin Province Science and Technology Research Project No. 20140520119JH, and project supported by State Key Laboratory of Luminescence and Applications.

Notes and references

1 S.-H. Liao, H.-J. Jhuo, P.-N. Yeh, Y.-S. Cheng, Y.-L. Li, Y.-H. Lee, S. Sharma and S.-A. Chen, *Sci. Rep.*, 2014, **4**, 6813.
2 Y. Liu, J. Zhao, Z. Li, C. Mu, W. Ma, H. Hu, K. Jiang, H. Lin, H. Ade and H. Yan, *Nat. Commun.*, 2014, **5**, 6293.
3 Z. He, B. Xiao, F. Liu, H. Wu, Y. Yang, S. Xiao, C. Wang, T. P. Russell and Y. Cao, *Nat. Photonics*, 2015, **9**, 174.
4 S. K. Hau, H.-L. Yip and A. K.-Y. Jen, *Polym. Rev.*, 2010, **50**, 474.
5 L.-M. Chen, Z. Hong, G. Li and Y. Yang, *Adv. Mater.*, 2009, **21**, 1434.
6 Z. He, C. Zhong, S. Su, M. Xu, H. Wu and Y. Cao, *Nat. Photonics*, 2012, **6**, 591.
7 J. M. De, I. L. Van and V. M. De, *Appl. Phys. Lett.*, 2000, **77**, 2255.
8 K. Wong, H. Yip, Y. Luo, K. Wong, W. Lau, K. Low, H. Chow, Z. Gao, W. Yeung and C. Chang, *Appl. Phys. Lett.*, 2002, **80**, 2788.
9 Y. Sun, J. H. Seo, C. J. Takacs, J. Seifter and A. J. Heeger, *Adv. Mater.*, 2011, **23**, 1679.
10 S. K. Hau, H.-L. Yip, N. S. Baek, J. Zou, K. O'malley and A. K. Y. Jen, *Appl. Phys. Lett.*, 2008, **92**, 253301.
11 T. Stubhan, N. Li, N. A. Luechinger, S. C. Halim, G. J. Matt and C. J. Brabec, *Adv. Energy Mater.*, 2012, **2**, 1433.
12 J.-C. Wang, W.-T. Weng, M.-Y. Tsai, M.-K. Lee, S.-F. Horng, T.-P. Perng, C.-C. Kei, C.-C. Yu and H.-F. Meng, *J. Mater. Chem.*, 2010, **20**, 862.
13 X. Li, F. Xie, S. Zhang, J. Hou and W. C. H. Choy, *Light: Sci. Appl.*, 2015, **4**, e273.
14 W. Qiu, R. MüLler, E. Voroshazi, B. Conings, R. Carleer, H.-G. Boyen, M. Turbiez, L. Froyen, P. Heremans and A. Hadipour, *ACS Appl. Mater. Interfaces*, 2015, **7**, 3581.
15 C. Tao, S. Ruan, G. Xie, X. Kong, L. Shen, F. Meng, C. Liu, X. Zhang, W. Dong and W. Chen, *Appl. Phys. Lett.*, 2009, **94**, 043311.
16 X. Fan, G. Fang, F. Cheng, P. Qin, H. Huang and Y. Li, *J. Phys. D: Appl. Phys.*, 2013, **46**, 305106.
17 J.-S. Huang, C.-Y. Chou, M.-Y. Liu, K.-H. Tsai, W.-H. Lin and C.-F. Lin, *Org. Electron.*, 2009, **10**, 1060.
18 W. Xu, Z. Kan, T. Ye, L. Zhao, W. Y. Lai, R. Xia, G. Lanzani, P. E. Keivanidis and W. Huang, *ACS Appl. Mater. Interfaces*, 2015, **7**, 452.
19 P. P. Boix, J. Ajuria, I. Etxebarria, R. Pacios, G. Garcia-Belmonte and J. Bisquert, *J. Phys. Chem. Lett.*, 2011, **2**, 407.
20 Z. Lin, C. Jiang, C. Zhu and J. Zhang, *ACS Appl. Mater. Interfaces*, 2013, **5**, 713.
21 S. Shao, J. Liu, B. Zhang, Z. Xie and L. Wang, *Appl. Phys. Lett.*, 2011, **98**, 203304.
22 F. J. Lim, A. Krishnamoorthy and G. W. Ho, *ACS Appl. Mater. Interfaces*, 2015, **7**, 12119.
23 V. D. Mihailetchi, P. W. M. Blom, J. C. Hummelen and M. T. Rispens, *J. Appl. Phys.*, 2003, **94**, 6849.
24 X. Jiang, H. Xu, L. Yang, M. Shi, M. Wang and H. Chen, *Sol. Energy Mater. Sol. Cells*, 2009, **93**, 650.
25 K. G. Lim, M. R. Choi, J. H. Kim, D. H. Kim, G. H. Jung, Y. Park, J. L. Lee and T. W. Lee, *ChemSusChem*, 2014, **7**, 1125.
26 Y. Park, V. Choong, Y. Gao, B. Hsieh and C. Tang, *Appl. Phys. Lett.*, 1996, **68**, 2699.
27 W. Song and M. Yoshitake, *Appl. Surf. Sci.*, 2005, **251**, 14.
28 J. Kwak, W. K. Bae, D. Lee, I. Park, J. Lim, M. Park, H. Cho, H. Woo, Y. Yoon Do, K. Char, S. Lee and C. Lee, *Nano Lett.*, 2012, **12**, 2362.

